

<https://doi.org/10.1038/s40494-026-02349-2>

The Pompeian ‘Blue Room’: in situ detection and economic estimation of Egyptian blue pigment in an ancient domestic sacrum



Mishaal A. Quraishi¹, Marco Nicola², James C. Weaver¹, Celestino Grifa^{3,4}, Valeria Amoretti⁵, Antonino Russo⁵, Gabriel Zuchtriegel⁵, Michael J. Tarkanian¹ & Admir Masic¹ ✉

Egyptian blue (EB) was a prized, intense blue pigment in antiquity, its color commonly associated with wealth, status, and divinity. While frequently used in small quantities for decorative enhancements, Pompeii’s newly excavated “Blue Room”, a shrine in *Regio IX Insula 10*, is remarkable in that the entire room is covered with this historically famous pigment. Using a combination of visible (white light)-induced luminescence, SEM-EDS, and Raman spectroscopy, we were able to spatially map the large-scale distribution of EB in situ, identify the method of application, and calculate the total quantity of EB used. We estimate that between 2.7 and 4.9 kg of EB was applied in the fresco technique, corresponding to a total cost of between 93 and 168 denarii. These findings demonstrate how modern multi-scale characterization tools can be employed to provide valuable insights into material investment, artistic practice, and social status in an ancient Roman domestic context.

Pompeii, like much of the ancient world, was a vividly colorful city. As it continues to be excavated, artworks such as frescoes, statues, and mosaics offer direct windows into the details of ancient Roman society. The preservation of the city’s original polychromy has yielded valuable insight into the materials and methods used by artists, as well as the economic standing of Pompeii’s inhabitants. One of the most well-known pigments in Pompeian art is Egyptian blue (EB)^{1–7}. Renowned as the first synthetic pigment in human history⁸, EB was manufactured as early as 3200–3300 BCE in Egypt as an alternative to the more expensive semi-precious lapis lazuli⁹.

Made by firing silica sand, calcium carbonate, copper-containing minerals, and alkali flux at ca. 850–950 °C, the cooled product is a glassy matrix interspersed with deep blue grains of calcium copper tetrasilicate (synthetic $\text{CaCuSi}_4\text{O}_{10}$, analogous to the rare naturally-occurring mineral cuprorivaite)¹⁰. In this paper, as in many archeological contexts, we use EB to refer more broadly to $\text{CaCuSi}_4\text{O}_{10}$ plus a heterogeneous mix of phases produced during its synthesis. These phases, with their mineral analogs in parentheses, include but are not limited to CuO (tenorite), low to high temperature SiO_2 polymorphs (quartz, tridymite, cristobalite), CaSiO_3 (wollastonite), and Cu-rich glasses¹¹. The color of EB is primarily derived from the $\text{CaCuSi}_4\text{O}_{10}$ crystalline phase¹², but a recent study shows that

samples with as little as 50 wt% $\text{CaCuSi}_4\text{O}_{10}$ can still exhibit a deep blue hue¹³.

In antiquity, EB was produced earliest in Egypt, Mesopotamia, and the Aegean^{14,15}. It became the most widely used blue pigment across the ancient Mediterranean and West Asia for over three millennia, despite the relative rarity of blue pigments compared to other colors¹. Blue often carried significant cultural associations, such as ties to status or divinity⁸. The value and prestige of EB have been debated, as some sources emphasize its use in elite contexts¹⁶ while others highlight how mass manufacture made it more accessible¹⁷. Over its long use history, EB’s value was not static.

Vitruvius also documented EB production in Puteoli (modern-day Pozzuoli, Italy) as early as the first century BC¹. Recent discoveries validate EB manufacture near Pompeii (Phlegraean area encompassing Puteoli)¹⁸. The proximity of Pompeii to the main EB production region for the Roman Empire is noteworthy. EB was typically traded in the Roman Empire as small pellets (*pilae*) of up to 20 mm in diameter that could be ground into usable pigment¹. While EB was the dominant blue pigment in Roman wall painting, other blues such as azurite, indigo, or lapis (from the mineral lazurite) were occasionally employed¹⁹. Within Pompeii, previous studies have spectroscopically identified EB in places such as the House of the

¹Massachusetts Institute of Technology, Cambridge, MA, USA. ²University of Turin, Torino, Italy. ³University of Sannio, Benevento, Italy. ⁴SHERIL, Samnium Heritage Innovation Lab, Benevento, Italy. ⁵Parco Archeologico di Pompei, Pompei (NA), Italy. ✉e-mail: masic@mit.edu



Fig. 1 | Location and interior of the Blue Room in Pompeii. **a** Pompeii Archaeological Park map site map with Regio IX highlighted in light blue, Insula 10 boxed in dark blue, and three additional regions marked with color-coded dots (Casa di Leda in red, Casti Amanti in orange, and Fontana Grande in green). **b** Color-coded plan

view schematic of Insula 10 (bakery: orange, laundry: pink, private domus: pale blue, Black Room (Room 24): gray, and Blue Room (Room 32): cyan). **c** Blue Room interior (left) and a magnified view of the southern/back wall (right).

Colored Capitals²⁰, the Temple of Venus²¹, the House of Garden²², and the House of Octavius Quartio²³.

The current gold standard diagnostic technique for characterizing EB is visible-induced luminescence (VIL) imaging, able to rapidly map EB across large (up to room-scale) areas, even identifying EB traces in places that no longer appear blue²⁴. In a typical VIL setup, a material is irradiated with visible light while a detector measures emitted near-infrared (NIR) light to map luminescence. Analyses are best performed indoors in a dark environment to minimize stray NIR interference, which can mask the EB signal. Recently, VIL-adapted night vision goggles (\$90–100 USD) were developed by Nicola et al.²⁵, which include a long band pass filter to block visible light and selectively map the NIR luminescence emitted by EB. This filtering method allows VIL imaging to be low-cost, portable, and rapid.

While these VIL goggles demonstrate significant advantages over spot-based analytical methods (e.g., portable spectroscopy techniques), the presence of high-intensity ambient sunlight (as would exist when examining EB-containing materials outdoors or in an active excavation site) significantly diminishes the detectable NIR EB signature, thus limiting their widespread application. To address this limitation, here, we report the development and use of an outdoor image subtraction method to mitigate the issue of stray NIR exposure from sunlight to identify EB using the goggles in daytime conditions. This approach was used to confirm the presence of EB (as opposed to other blue pigments which do not luminesce) at five excavation sites in Pompeii: Casa di Leda, Casti Amanti, and Fontana

Grande (Fig. 1a), the Black Room (Fig. 1b), and the focus of this paper, the Blue Room (Fig. 1b, c).

The Blue Room is a recently excavated and well-preserved shrine (measuring $\sim 2.7 \times 3.3$ m), within a private domus in the southern part of Regio IX Insula 10 in Pompeii²⁶. This room is notable for its remarkably high content of EB, covering nearly every exposed wall surface. Upon the recent completion of its excavation, the archeological site was discovered to contain the distinctively blue painted walls, multiple amphorae, and piles of construction materials situated exactly as they were moments before the eruption of Mt. Vesuvius in 79 CE²⁷.

With the shrine fully excavated, the present work aims to: (i) provide a survey of the different pigments employed in the ornamentation of the Blue Room, (ii) develop an in situ method for detecting EB under ambient light (sunlit) conditions, and (iii) develop methods for estimating the quantity of blue pigment employed in the construction of the Blue Room. In summary, this study aims to expand our understanding of ancient polychromy use and the artistic practices in Pompeii, particularly regarding the material and economic choices involved in the construction of elaborate spaces such as the Blue Room.

Method

EB sampling information and preparation details

All archeological sampling and analytical work was conducted under the 51956544MIT_ITALY (PA-POMPEII, 15/12/2023, CONVENZIONI

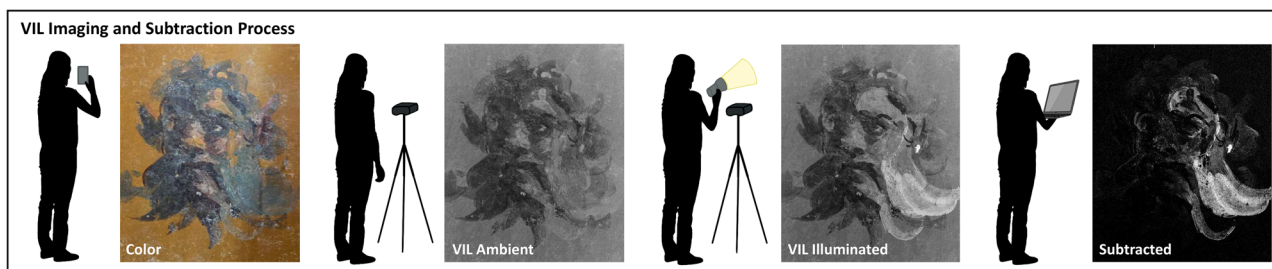


Fig. 2 | VIL Subtraction technique illustrated on a bearded figure from Casa di Leda. Left to right shows color image, environmental light (“VIL Ambient”), spotlight with a 70 W LED lamp (“VIL Illuminated”), and the final subtracted image. While in the

color image it may appear that the entire figure contains EB (purple tones may have been obtained through mixing EB with another pigment), VIL demonstrates that only certain regions contain EB.

ITALIA 62) agreement between the Parco Archeologico di Pompei and Massachusetts Institute of Technology, in full compliance with all required permits, local regulations, and best practices, ensuring provenance, transparency, and adherence to heritage protection laws. All samples were collected in Pompeii during the summer of 2024, and fall into two categories: dry reference (unprocessed) raw pigment from the official Pompeii Archeological Park collection (from prior excavations of Casa dei pittori al Lavoro, or the *House of the Painters at Work*), and new pigmented samples from the *Blue Room*.

Four reference EB pigment samples (Figs. 7 and 8) were collected from the *House of the Painters at Work*, a site that contained unfinished wall paintings and the raw materials used in their production (located in Casti Amanti marked with an orange dot in Fig. 1a). These samples represent the raw pigments directly employed by Pompeian artists and were used as references to quantify the ratio of Cu-containing to non-Cu-containing phases in Pompeii EB (Fig. 8). This ratio was then applied to calculate the total amount of EB used in the creation of the *Blue Room* (see Volume Fraction EB section below).

Three small, pigmented fragments from the *Blue Room* (BR01, BR02, BR03; Figs. 9–11) were obtained from two locations within the shrine: the cornice (BR01) and the wall (BR02 and BR03). These millimeter-sized samples were manually extracted from larger fragments (centimeter-scale) that had become detached from the room during previous excavations. The larger fragments currently remain in storage in Pompeii.

All samples were either analyzed in situ (on the wall at the archeological site), analyzed as isolated fragments in their native state (e.g., BR01 and BR02 in Figs. 9 and 11), or resin-embedded and imaged as polished cross-sections (e.g., BR03 in Figs. 9–11).

For the preparation of polished sample cross-sections (e.g., Sample BR03), the fragments were embedded using Buehler Epothin 2 Resin with Epothin Hardener (2:1 mixing ratio) and cast into 1-inch diameter round molds. The samples were progressively ground down using silicon carbide papers of 240, 400, and 600 grit to reveal the embedded material. The resulting cross sections were further polished to a 1 μm finish using diamond paste, micropads from Pace Technologies, and mineral oil. Final polishing was performed with a 0.1 μm diamond polishing disc (with distilled water).

In situ pigment characterization

A preliminary investigation of the *Blue Room*'s pigment palette was carried out and followed a micro-invasive (multi)analytical protocol already tested on Pompeian wall paintings and other archeological contexts in the region^{16,23,28,29}. These techniques (each outlined below) provided an initial non-invasive chemical survey of the major pigments in the room.

Optical micrographs of the different pigmented regions (Fig. S2) were acquired with a Dino-Lite digital microscope with a magnification range of $\times 20$ – $\times 220$.

The qualitative elemental composition for each pigment (Fig. S2) was measured on areas of 3 mm (spot diameter) using a portable Bruker TRACER 5G X-ray fluorescence (pXRF) spectrometer. For comprehensively identifying the chemical elements, both a HighZ (30 kV, 15 μA , 20 s)

and LowZ (15 kV, 16 μA , 30 s) presets were employed, for elements with both high and low atomic numbers, respectively. The spectra were processed with the ARTAX Spectra 8.0.0.476 software package (Bruker AXS Handheld, Inc.).

Fourier transform infrared spectroscopy (FTIR) in attenuated total reflectance (ATR) mode (Fig. S2) was performed with a portable BRUKER Alpha FTIR spectrometer, in a spectral range between 4000 and 400 cm^{-1} . The spectra, acquired by using 64 scans for each run, had a resolution of 4 cm^{-1} , and were processed using the Bruker Opus 7.8 software package.

VIL image subtraction to identify EB

Non-invasive field analysis was conducted using VIL imaging to map EB distribution across the *Blue Room*'s wall surfaces. VIL, described by Verri 2009³⁰, is widely used in museums and laboratories to detect EB's unique NIR emissions. However, challenges remain with stray NIR from synthetic and natural light sources. Whilst indoors, stray NIR can often be eliminated or mitigated by using filters³¹. However, Triolo et al. notes that, in some cases, small amounts of parasitic IR reflectance (generated from a camera flash or LED), can be helpful for the spatial localization of EB on artifacts³¹. In their study, conducted indoors using a modified camera, they present a way to correct for the parasitic IR using image subtraction³¹. For outdoor contexts, VIL cameras have been limited to nighttime operation to avoid daylight NIR³². However, in sites like Pompeii, night access is often not possible, and ambient daytime light cannot be fully eliminated.

To address these limitations, this study introduces and applies an outdoor image subtraction method (Fig. 2). First, two distinct images were acquired with modified night vision goggles (Salati brand goggles modified with a DHD Digital 43 mm long-pass IR850 filter, see Nicola et al.)²⁵. One image was taken under natural light conditions (referred to as “VIL Ambient”) and another directly after with LED spotlight illumination (“VIL Illuminated”). An LED lamp with low emission in the IR range was used (NEEWER CB60B 70 W LED Video Light with 2.4 G/APP Control). This light source was chosen for its low cost, ease of use in the field, and high wattage to provide sufficient excitation from EB. We acknowledge this system generates a small amount of parasitic IR, which for our purposes (larger-scale EB confirmation) aided as a spatial reference³¹, as shown through pairing the VIL images with their full-color counterparts. Images were aligned in Adobe Photoshop and saved as high-quality jpg files to match the native image format from the goggles. To obtain a final EB map, a Python script used the OpenCV library and was run in the Spyder environment to subtract corresponding pixels of the “VIL Ambient” image from the “VIL Illuminated” image. After subtraction, image brightness was increased in Photoshop for clarity, but no other post-processing was done. Note that the brightness of the VIL signal cannot be quantitatively correlated to the amount of EB present due to variances in natural lighting conditions, spotlight intensity, and subjective applications of image-specific post-processing.

EB sample characterization

Optical images of the prepared cross section (Fig. 9 bottom row, 10, and 11, and Supplemental Figs. 5–7) were taken with an Olympus DSX1000 digital

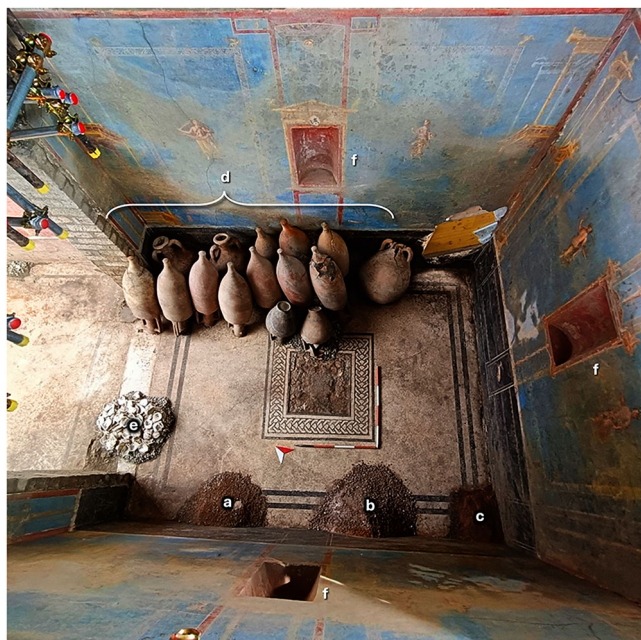


Fig. 3 | Aerial view of the Blue Room containing. a–c Piles of construction materials, d transport amphorae, e a pile of oyster shells (of unknown function), and f niches with red-painted interior. Image adapted with permission²⁷.

microscope using a $\times 10$ objective under polarized light. The lower magnification optical micrographs (Figs. 7 and 8) were acquired with a Keyence VHX-2000 digital microscope.

Semi-quantitative SEM-EDS was utilized to better understand sample elemental composition, morphology, and heterogeneity. Both native and polished samples were imaged using a Tescan Vega GMU scanning electron microscope in low vacuum (15 Pa) at 20 keV equipped with a dual detector EDS system. EDS elemental maps and their corresponding ternary diagrams were acquired using the Bruker Esprit software package.

Raman spectroscopy was conducted on section BR03 (Fig. 10) using a WiTec Alpha 300R confocal Raman microscope equipped with a Nd:YAG 532 nm laser, a 600 g/mm grating UHTS Raman Spectrometer (WITec, Germany), and a CCD-camera cooled to -60 °C. Excitation wavelengths were calibrated to match the T_{2g} mode peak of a silicon wafer to 520 cm^{-1} . WiTec Project 5 software was used to perform background subtraction. The Project 5 k -means clustering function was used to identify spectral components, which were matched to mineral patterns using CrystalSleuth software and compared to references from the RRUFFTM database.

EB pigment estimation

The total mass of EB used in the Blue Room was estimated using the following Eq. (1):

$$\begin{aligned}
 &(\text{EB painted surface area}) \times (\text{Average EB - containing layer thickness}) \\
 &\quad \times (\text{volume fraction EB}) \times (\text{EB density}) = \text{EB mass} \quad (1)
 \end{aligned}$$

EB painted surface area (m^2) was determined using a standard length \times width formula for each feature of the room (Table S1). Average EB-containing layer thickness (μm) was estimated using fifteen points spaced along cross-section BR03 (Fig. S9). These measurements were normally distributed, and as such, the mean thickness and standard deviation were reported. EB painted surface area \times average EB-containing layer thickness represents the volume of the average EB-containing layer in the Blue Room. It is important to note, however, that this volume is not completely filled with EB, as the pigment layer also contains the fresco plaster (calcium-based

matrix). We therefore scaled our volume calculation using an estimated Volume Fraction EB.

Two different estimations were made for the Volume Fraction EB (VF1 and VF2). The first, VF1, was calculated using the unembedded wall fragment BR02 (Fig. 9, column d middle). The isolated Cu elemental map for BR02 (which covered an area measuring 1 mm by 1 mm) was analyzed using the ImageJ software package to determine the percent area of Cu-containing phases (Fig. 11a). More specifically, in ImageJ, the Cu map was binarized, de-speckled, and thresholded so that the area of all particles $>1\ \mu\text{m}^2$ were measured using the *Analyze* function (particles smaller than $1\ \mu\text{m}^2$ were presumed to be noise, and as such, were excluded from these calculations). The resulting percent area was scaled up by the ratio of Cu-containing to non-Cu-containing EB phases found in the *House of the Painters* EB reference samples (Fig. 8).

The total EB area fraction was approximated to represent its volume fraction according to ASTM metallurgy methods for analyzing heterogeneous materials. Specifically, method E562 assumes that the two-dimensional area fraction observed in a section corresponds to the three-dimensional volume fraction when particles are equiaxed and randomly distributed³³. Although EB particles are not perfectly spherical, the average particle population was treated as equiaxed. Volume fraction 2 (VF2) was calculated from cross section BR03 using optical images and three $400 \times 400\ \mu\text{m}$ EDS maps (Fig. 11b). The Cu-containing area was also estimated with ImageJ by binarizing, de-speckling, and thresholding the maps, and then dividing the Cu-rich area by the total pigment layer area (manually measured with the ImageJ *Area* function using the optical micrograph as a guide). These two approaches (VF1 and VF2) provide lower and upper bounds for estimating the EB volume fraction in the Blue Room.

EB density (g/cm^3) was used to convert this volumetric measurement into EB mass (g). The estimated density of EB was $3.08\ \text{g/cm}^3$ (the reported density of $\text{CaCuSi}_4\text{O}_{10}$ from the Mindat mineral database: <https://www.mindat.org/min-1189.html>).

Results

Excavation history and contents of the Blue Room

The Blue Room is part of a private residence in *Regio IX Insula 10*²⁷. Note that areas in Pompeii are designated by a naming scheme of *Regio* (Region), *Insula* (Block), Room, e.g., *Blue Room: IX.10.32*. Multiple other structures (Fig. 1b) have been discovered in the same *insula*, such as a laundry facility and a bakery, which was likely operated through slave-based labor³⁴. The living quarters, containing the Blue Room (shaded cyan in Fig. 1b), include a thermal bath complex (Room 47), central courtyard garden (Area 19), staircase (Area 25) leading to an upper level, and an elaborate dining hall (Room 24)²⁷. This banquet hall, known now as the *Black Room* due to its wall color, could have accommodated 20–30 guests and has a white tiled mosaic floor. Its walls are decorated with paintings and inscriptions (several names and phrases), suggesting the residents were literate, a significant detail given low literacy rates in Pompeii³⁵. These combined architectural and decorative factors suggest that the owners of the *domus* were of high social standing.

The Blue Room itself is accessed through one entry point, a roofed and decorated vestibule (Room 31 in Fig. 1b), which is connected to the central courtyard (Area 19 in Fig. 1b)²⁷. Stratigraphic analysis suggests that the Blue Room is on the ground floor, and there was a room with a wooden floor above it. The deposition of ash suggests that volcanic material during the 79 CE eruption entered the room from the garden and antechamber as it flowed from north to south²⁷. During the 18th or 19th century (Bourbon period), tunnels were used to breach the room, and these excavators left behind two jugs and two lamps in the tunnels. This prior breach likely explains why ritualistic objects were not found in the room during recent excavations, despite it likely having a sacred function²⁷.

Subsequent excavations have now fully revealed the contents of the Blue Room (Fig. 3). Along the western wall, there were three piles containing crushed ceramic fragments (*cocciopesto*), a pile of lime grains, and volcanic ash (*pozzolana*). These materials were likely used for construction or restorations of nearby areas that may have been damaged by volcanic and

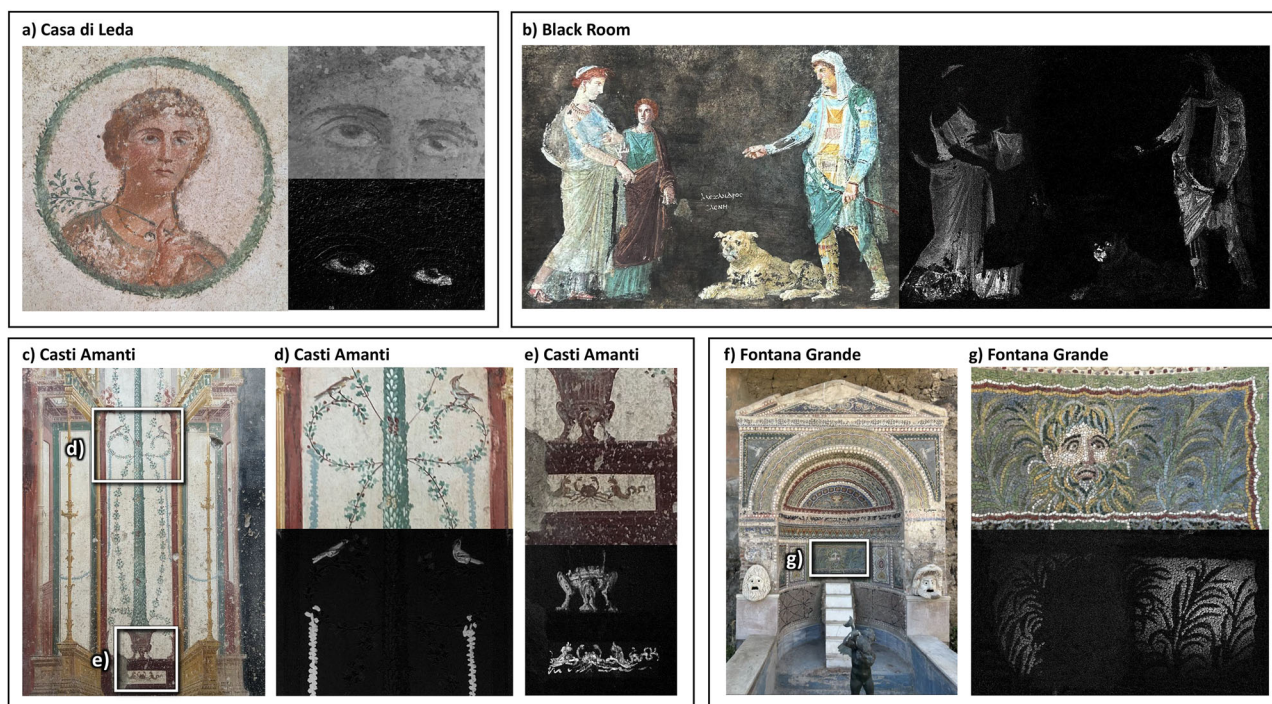


Fig. 4 | EB identified at multiple locations in Pompeii. a Portrait medallion in Casa di Leda with EB in the eyes. **b** Portrait from the *Black Room* with EB in robes and face of a dog. **c** Color image of a decorative pillar in Casti Amanti. **d** Bird and garland

identified as EB. **e** Crab and pillar base detail identified as EB. **f** Fountain in Casa Della Fontana Grande. **g** color and VIL image of EB tesserae surrounding the face in the fountain.

seismic activity prior to the 79 CE eruption²⁷. Fifteen transport amphorae lean against the eastern wall, mostly overturned, suggesting that they have been recently washed and were ready for reuse²⁷. In other parts of the *domus*, amphorae have been found containing lime, which was likely intended for construction purposes²⁶. Towards the entrance of the room, there is a pile of oyster shells (*Ostrea edulis*), but their function is currently unknown. The entire floor is a tiled mosaic with the outer double lines of black and an inner square pattern with a braided motif in the center of the room. The very center of the mosaic was damaged during the Bourbon period breach²⁷.

The artwork in the *Blue Room* is attributed to the *Fourth Style* of Roman wall painting, the final and most elaborate of the traditional chronological schemes³⁶. *Fourth Style* frescoes are characteristic of the mid-first century CE, particularly in houses renovated or newly constructed after the earthquake of 62 CE²³. This stylistic association may therefore provide a chronological context for the *Blue Room's* creation. On each of the three larger walls, central red niches (Fig. 3f), likely used for offerings, are flanked by two inwardly facing female goddess figures. Of the six painted figures (Fig. S3), four represent the different seasons, and two are allegories of agriculture and pastoralism. The seasons are a commonly depicted motif in other artworks in Pompeii²⁷.

The *Blue Room* walls also feature painted golden-colored pavilions, candelabra, and fantastical creatures such as sphinxes and winged griffins. The artistic imagery references idealized agrarian life and prosperity, signifying the aristocracy's disconnect from the working class. The elites who lived in this *domus* would have likely not participated in manual labor, but instead, were likely profiting off of slave labor from places such as the many villas and wineries of the countryside (see literary discussion in Zuchtriegel et al.²⁷).

Initial screening of the *Blue Room's* fresco pigments

Since the room was newly excavated in the summer of 2024, no modern restorations or interventions have been carried out on the polychrome frescoes. Preliminary micro-invasive investigations using portable ATR-FTIR and pXRF instruments were employed to characterize the main pigments used in the decoration of the room.

The blue pigment (Fig. S1) covers the largest surface area in the room, and pXRF analysis shows high concentrations of calcium and copper, consistent with the presence of EB, along with smaller quantities of silicon and minor peaks attributed to potassium, strontium, and iron.

The red pigment is the second most widespread hue in the room (e.g., in the votive niche, red point, Fig. S1). It appears as a compact red layer, on which sporadic black and whitish spots were observed (Fig. S2). The pXRF spectra reveal intense Fe–K lines, together with signals of Ca, S, Sr, K, Cu, Pb, and Si. ATR-FTIR confirmed the presence of iron oxides, showing the characteristic Fe–O vibrations at 526 and 466 cm^{-1} , along with calcite bands at 2512, 1795, 1406, 872, and 712 cm^{-1} , and silicate stretching and bending modes at 1012 cm^{-1} . These results suggest the use of an earth pigment containing silicates, namely red ochre. The occurrence of Pb in pXRF spectra may suggest the minor addition of lead red in the pigment mixture.

The green pigment was mainly used for decorative patterns (green point, Fig. S1), and shows significant concentrations of iron along with a minor potassium peak (Fig. S2). The ATR-FTIR spectrum, with a peak at $\sim 1600 \text{ cm}^{-1}$ and a broad band between 3000–3500 cm^{-1} , suggests the pigment derives from minerals such as celadonite or glauconite. As shown in the optical micrograph, tiny EB particles are scattered within the green pigment, suggesting a mixture of green earth with small quantities of EB. The preliminary investigation revealed that EB was not only the most widely used pigment in the room, but was also added in minor or trace amounts to other pigments to enhance the vividness of the wall paintings²⁹.

The yellow pigment was applied to create the frame of columns (yellow point, Fig. S1). As revealed from optical microscopy (Fig. S2), the yellow areas show coarser EB grains, white inclusions, and rare tiny red particles, indicative of the use of a mixture of coloring agents. Chemically, Ca dominates, while Fe is also present, together with minor Cu and traces of S, Si, K, and Sr. The ATR-FTIR spectrum highlights bands of goethite ($\alpha\text{-FeOOH}$) (1627, 913, and 797 cm^{-1}), kaolinite (3695, 3621, 1114, 1030, 1008, 755, 670, 600, 533, 468 cm^{-1}), and calcite (2519, 1795, 1414, 873, 712 cm^{-1}).

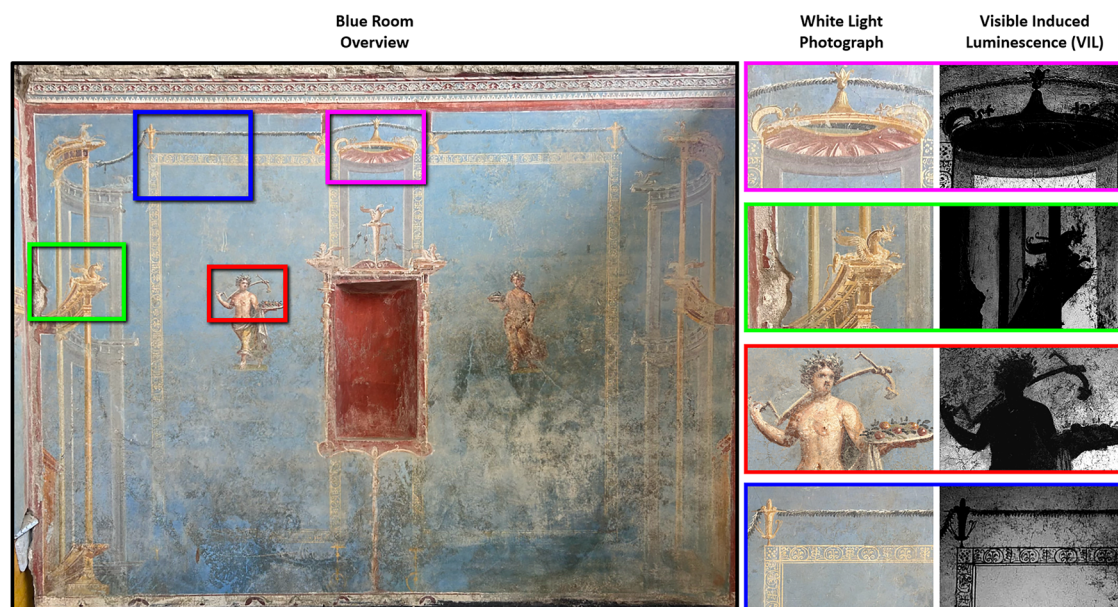


Fig. 5 | Selected VIL of painted decorations inside of the Blue Room. Southern wall (left), selected sections (middle) with VIL images (right) taken using our image subtraction method.

Identification of EB using VIL goggles and image subtraction

While EB was identified using portable VIL goggles (Fig. 4) at multiple excavation sites in Pompeii (Fig. 1a and b), particular attention was given to its extensive use in the *Blue Room*, where our analysis aimed to estimate the cost of painting such a space (one presumably accessible only to an elite audience, rather than the general public).

The use of portable VIL instrumentation in daylight represents a key advancement in non-invasive field analysis of EB. The image subtraction method developed here now enables EB identification in nonideal conditions without the need to perform experiments at night, invasively sample, or shield ambient NIR from the sun. Figure 4 shows selected results from detecting EB in Casa di Leda (*House of Leda* V.6.12), the *Black Room* (IX.10.24), Insula dei Casti Amanti (including Casti Amanti *House of the Chaste Lovers* IX.12.6 and the nearby Casa dei Pittori al Lavoro *House of the Painters at Work* IX.12.9), and Casa Della Fontana Grande (*House of the Great Fountain* VI.8.22).

Artists also applied EB to the whites of the eyes to impart a subtle bluish-gray tint, adding depth and enhancing realism. This technique, previously identified in other ancient portraiture²⁴, can be seen in Fig. 4a in a medallion of a bejeweled female figure holding an olive branch. EB was also detected in the eyes and face of a dog painting from the *Black Room* banquet hall, as shown in Fig. 4b. This scene depicts a meeting between the abducted Helen of Sparta (Helen of Troy) and Paris³⁵. EB is seen in all three figures' clothes as part of multiple blue and green tones. The use of EB in the *Black Room*, given its close proximity to the *Blue Room*, is particularly significant, as the owners used EB in multiple parts of the *domus*. In Casti Amanti (Fig. 4c), VIL imaging clearly demonstrates that EB was used both by itself (Fig. 4d) and mixed to create shades of purple (Fig. 4e).

EB was also used to form mosaic tesserae³⁷, and Casa della Fontana Grande is a clear example of a first-century-CE fountain using this technique (Fig. 4f and g). The fountain, with its blue tiling and embedded seashells, looks very similar to one found in Casa del Granduca di Toscana (*House of the Grand Duke of Tuscany*, VII.4.56 from CE 35-50)³⁷. This parallel suggests spaces like these (ones featuring EB) held similarly high levels of prestige. Our VIL analysis revealed that EB coated the base of the fountain and comprised the tesserae surrounding the main face mosaic, including stripes on the side of the fountain's front, but not the darker blue tesserae, which are likely a copper or cobalt-containing glass³⁸ (Fig. S4).

The successful detection of EB through VIL in these varied architectural contexts, from wall paintings to fountain decoration, opens new

avenues for rapid *in situ* pigment documentation, particularly in outdoor sites. The locations discussed above are within private structures (not public infrastructure), and the use of EB in these areas supports the idea that polychromy was not merely aesthetic, but communicated messages of wealth, refinement, and cultural aspiration (this topic of color selection in Roman homes is further discussed by Clarke³⁹).

Identification of EB in Blue Room using VIL subtraction

The most unusual aspect of the *Blue Room* is the distinctive blue color of its walls. VIL imaging with the goggles and our new subtraction method confirmed that EB was the likely background pigment (Fig. 5), which was further validated with subsequent SEM-EDS and Raman spectroscopy studies (see Figs. 7–10).

Where surface layers have degraded, EB is visible underneath, with its signal detected by VIL imaging (Fig. 6b). While notably, in areas covered by thicker red, white, or yellow pigments, the emission is blocked, these results clearly demonstrate that the walls were first painted entirely with a base layer of EB prior to the application of additional decorations.

Reference EB characterization

Raw reference EB samples were further analyzed using scanning electron microscopy (SEM) and energy-dispersive X-ray spectroscopy (EDS) to visualize morphology, atomic composition, and elemental distributions. First, large-area elemental mapping was conducted on a small, fully intact pellet of pigment acquired from the *House of the Painters at Work* (Fig. 7).

EDS maps on a dark blue (raw) reference pellet show a heterogeneous chemical composition with particles of variable grain sizes, with individual grains varying in calcium, silicon, and copper content. The ternary phase diagram plots the compositions of point measurements made across the surface of the pellet, as a function of relative calcium, silicon, and copper concentrations. These EDS data clearly demonstrate that EB is a heterogeneous mixture of several blue and non-blue, Cu-containing and Cu-free phases, over a wide range of chemical compositions⁴¹, an observation consistent with many previous reports describing the compositional heterogeneity of EB^{13,15,40,41}.

The embedded raw reference pigment samples displayed various shades of blue (see optical micrographs in Fig. S5–S7), as well as heterogeneous distributions of Ca, Cu, and Si. The elongated and sometimes striated morphology of the CaCuSi₄O₁₀ crystals (colored purple in Fig. 8, column b) intermixed with Ca-rich and Si-rich phases (red and green in

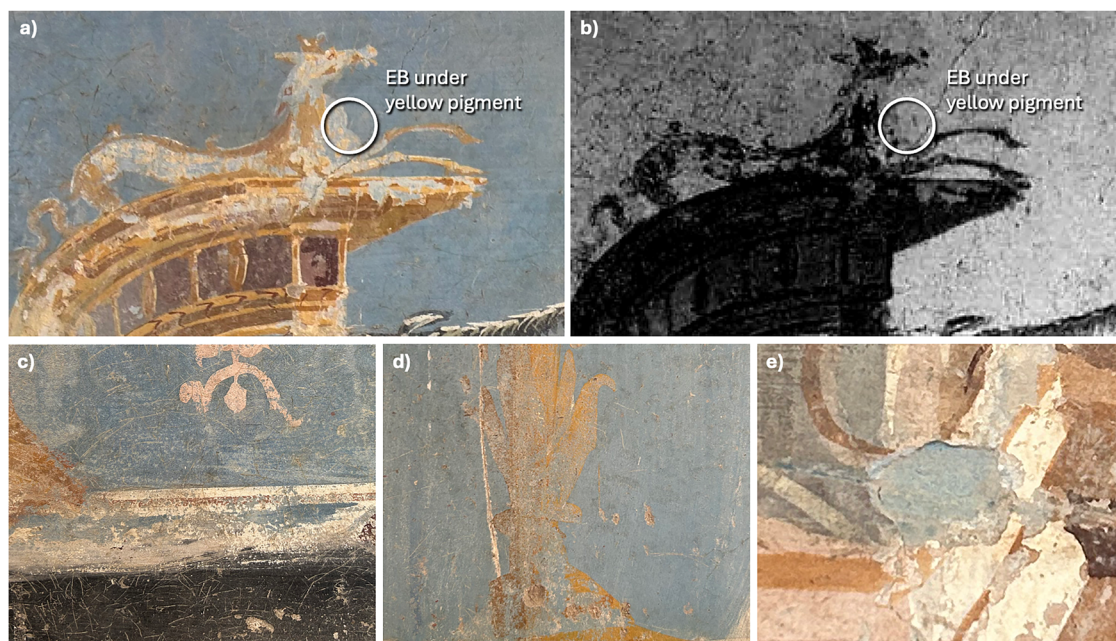


Fig. 6 | EB base layer confirmed optically and with VIL. **a** Color photograph of the dragon detail on the top left of the southern wall. **b** VIL image demonstrating that the EB signal shows through the degraded yellow paint. **c–e** Selected examples where EB is clearly visible under other pigments.

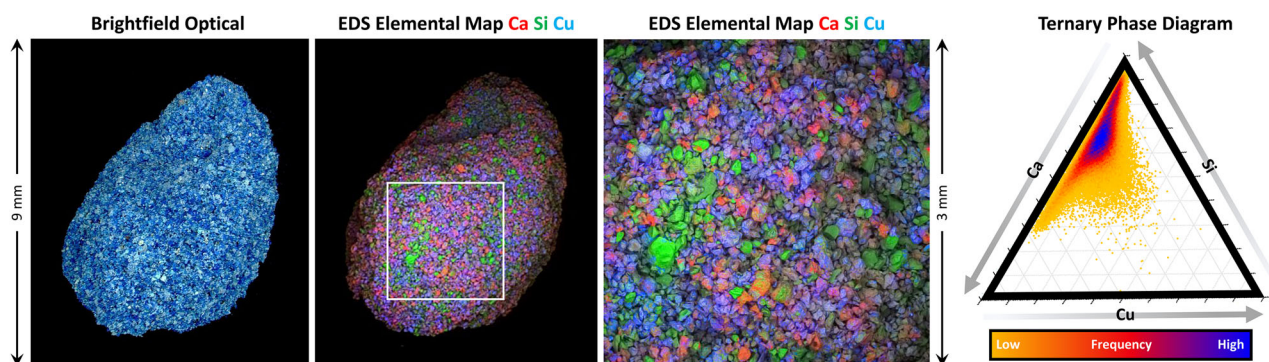


Fig. 7 | Raw reference pigment pellet characterization. Brightfield optical micrograph (left) and elemental maps (middle two images) of a pellet of EB from the *House of the Painters at Work*. The ternary diagram (right) generated from the EDS mapping data clearly shows the compositional heterogeneity of the native (raw) pigment.

Fig. 8, column b) appears very similar to that reported previously (see Fig. 6 in Tite et al.⁴² and Fig. 5 in Arletti et al.³⁸). The binarized copper maps (Fig. 8, column c) were used as a baseline to estimate the area percentage of the EB sample that was Cu-containing (the non-Cu-containing phases were determined by 100%–(Cu-containing%). To provide an accurate compositional ratio, only the area from the pigment (i.e., no epoxy) was counted (outlined in orange in Fig. 8, column b).

Blue Room sample characterization

Three different EB samples from the *Blue Room* (Fig. 9) were analyzed (and compared to the raw EB reference samples). The cornice sample (top row BR01) contains grains that exhibit a distinctive dark blue shade as observed via optical microscopy (Fig. 9, columns a and c), which are similar to the raw pigment reference sample shown in Fig. 7. This dark blue also correlates to higher relative copper signals, and thus higher copper content, as is clearly illustrated in the EDS maps (Fig. 9, column b).

Dark blue particles of the same shade are visible in the wall samples (Fig. 9, column c), but are present in far fewer numbers. This distribution is reflected both in the optical micrographs, the EDS maps (Fig. 9, column d), and the ternary phase diagrams (Fig. 9, column e). The sparseness of blue particles implies less copper content overall, and accordingly, the ternary

phase diagrams exhibit pronounced reductions in copper content and increased levels in calcium content for the wall fragment in the middle row (in comparison to the cornice fragment in the top row). Because fewer dark-blue particles are dispersed through the wall paint, the surface appears to be a paler sky-blue color, even though each grain is chemically and chromatically similar to those in the cornice. Whether the lower loading of EB in the wall reflects economy or a deliberate preference for a lighter background remains unclear.

In every specimen in Fig. 9, the underlying plaster (*intonaco*) is dominated by calcium with lesser amounts of silicon-rich materials, most clearly displayed in the EDS map of BR03 (Fig. 9, column b bottom). The ternary plot for the raw pigment reference pellet (Fig. 7) overlaps with the copper-rich field of the cornice sample (Fig. 9, column e upper), whereas the wall sample plot (Fig. 9, column e lower) shifts toward the calcium apex, mirroring the dilution of EB by the calcitic matrix noted above. The optical micrographs, EDS maps, and ternary diagrams therefore converge on a single conclusion: the walls and cornice were painted with the same EB pigment, but the walls received it at a much lower particle density, allowing the Ca-rich plaster to dominate the composite signal and the perceived color.

Further targeted characterization on section BR03 was performed on the region with the largest EB grain to identify the adjacent mineral phases in

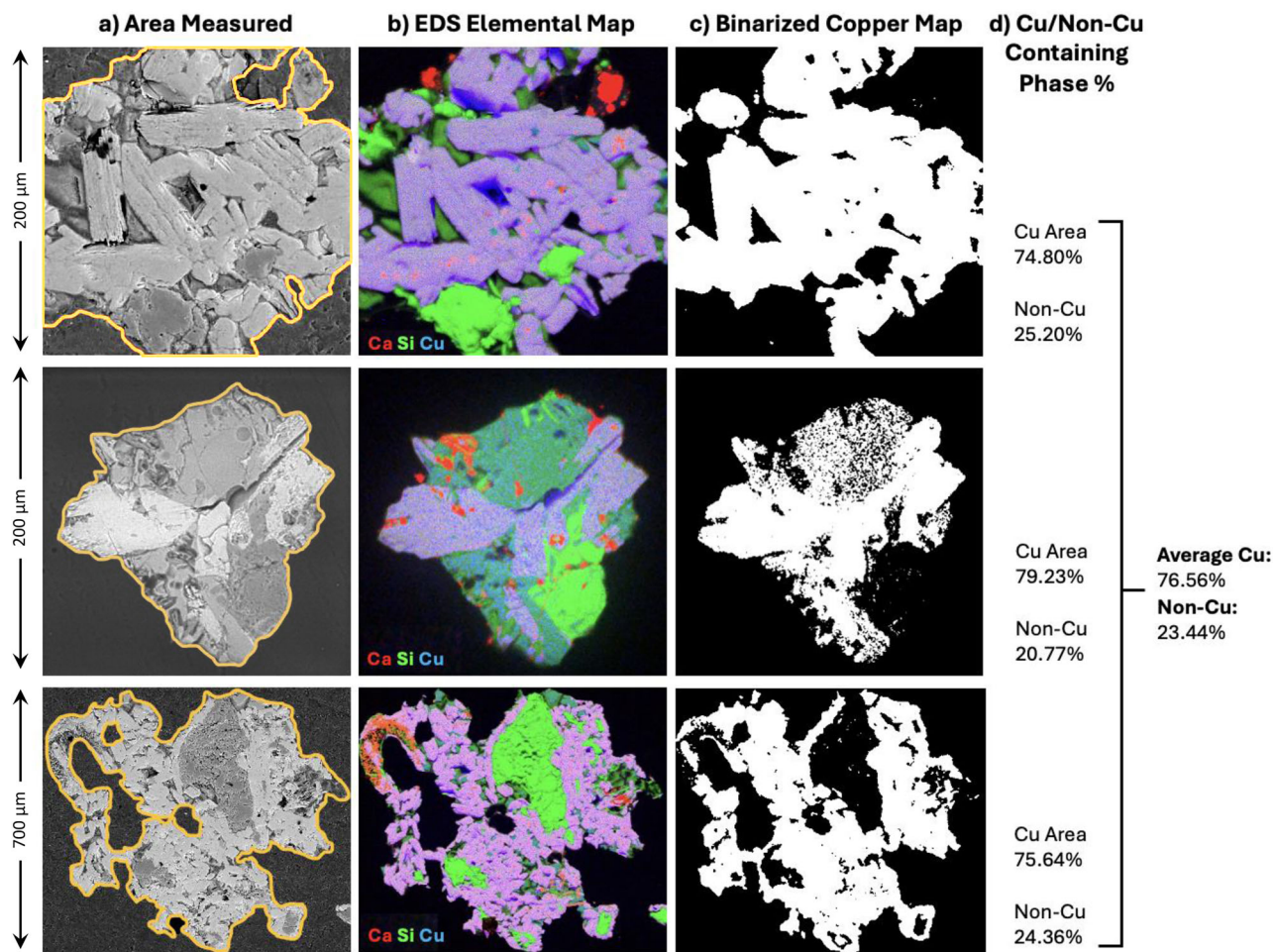


Fig. 8 | Determination of the volume fraction of Cu-rich phases in EB. Each row shows a different embedded and polished raw pigment sample acquired from the *House of the Painters at Work*. **a** Backscattered electron micrograph with the measured area outlined in orange. **b** Corresponding EDS elemental maps (Ca, Si, Cu). **c** Binarized Cu maps and **d** calculated area percentages of Cu- and non-Cu-containing phases (average values reported on the right).

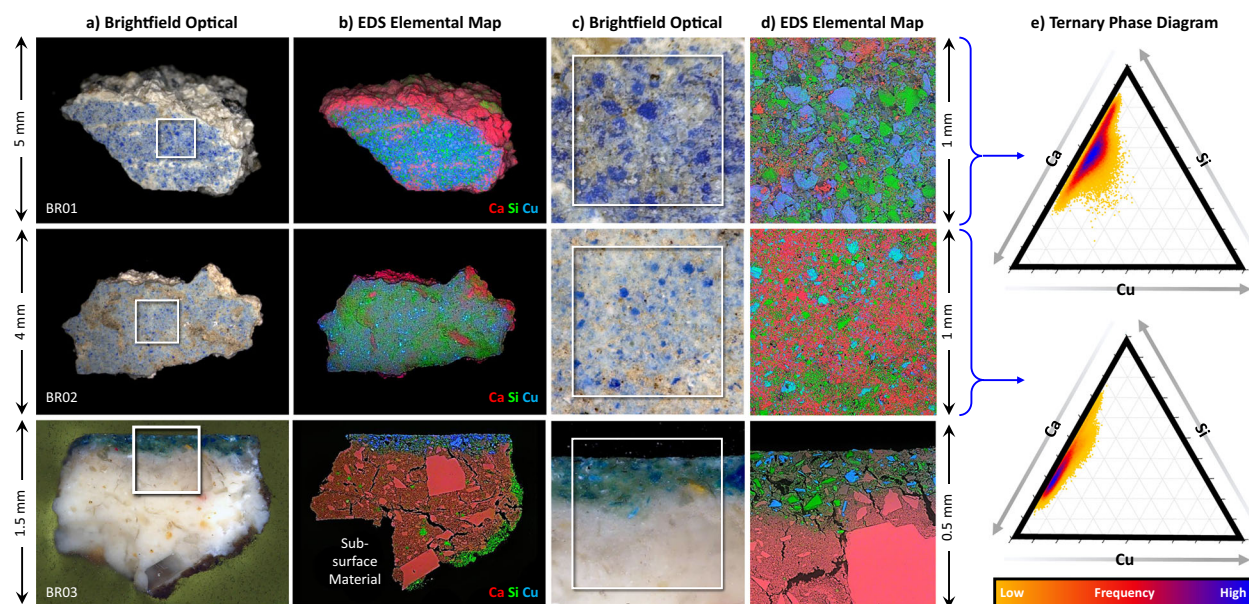


Fig. 9 | Elemental distributions in the Blue Room samples. Three rows (top to bottom) show an unembedded cornice sample, an unembedded wall fragment, and an embedded wall fragment from the *Blue Room*. Column **a** displays brightfield optical micrographs with their corresponding elemental maps in column **b**. Column **c** shows a higher magnification optical micrograph of each sample, with their corresponding elemental maps in column **d**. The rightmost region of the figure, column **e**, shows ternary diagrams of the two unembedded samples, mapping their relative concentration of Ca, Si, and Cu.

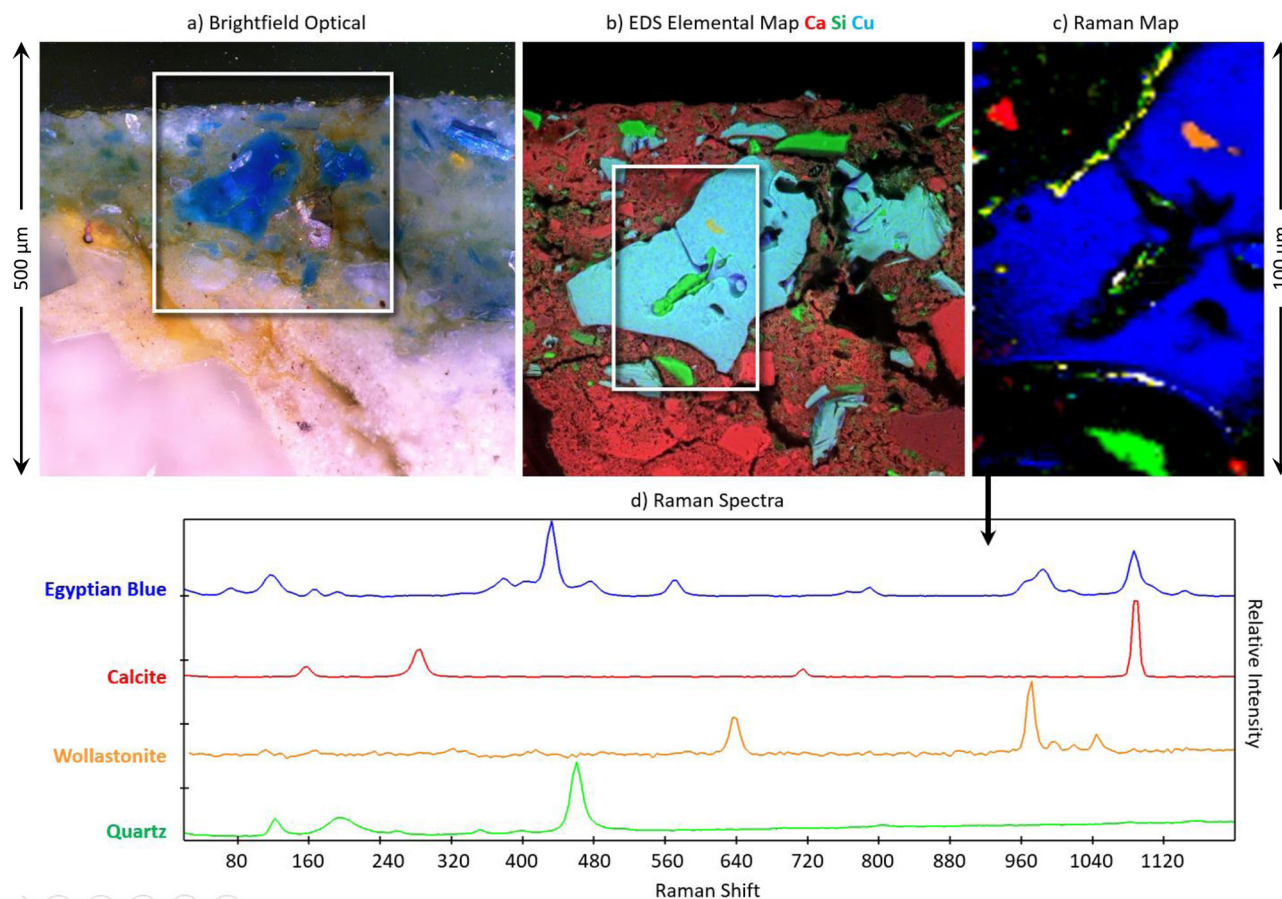


Fig. 10 | Analysis of an EB grain from the wall cross-section BR03. **a** Brightfield optical micrograph of BR03, highlighting the largest blue particle, and its corresponding EDS elemental map **b**. **c** Raman map differentiating phases as EB (blue),

calcite (red), quartz (green), wollastonite (orange), and fluorescence from the matrix (yellow), and their corresponding Raman spectra **d**.

the *Blue Room* wall. Brightfield optical microscopy shows the area's coloration (Fig. 10a), and its corresponding EDS map displays the elemental distribution of Ca, Si, and Cu (Fig. 10b). EDS reveals that, as expected, the darker blue grains in the optical micrograph are Cu-rich. To identify the specific phases present, Raman spectroscopy was employed. Raman mapping (Fig. 10c) and spectra (Fig. 10d) revealed the definitive presence of $\text{CaCuSi}_4\text{O}_{10}$ (432 cm^{-1}), CaCO_3 (calcite, 1086 cm^{-1}), CaSiO_3 (wollastonite, β phase $636, 969.5, 1042\text{ cm}^{-1}$), and SiO_2 (quartz, α phase exhibits strong bending mode around 464 cm^{-1}), an observation consistent with previous EB studies⁴³. Note that β -wollastonite is a naturally occurring phase formed at lower temperatures than the α -wollastonite¹¹, revealing that temperatures did not likely exceed $1125\text{ }^\circ\text{C}$ during the EB firing process⁴⁴. Prior research has also described a light blue-green phase termed “cupro-wollastonite,” which may be present in section BR03. However, both this and previous studies have noted that β -wollastonite and cupro-wollastonite cannot be clearly distinguished by methods employed in the present study¹¹.

Estimation of the total mass of EB pigment employed in the *Blue Room*

EB is a highly heterogeneous material with particles rich in Ca, Cu, and Si intermixed on the sub-micron scale. This heterogeneity, combined with the fresco painting technique, where pigment mixed with water is pushed directly into wet lime plaster, makes it difficult to precisely distinguish EB pigment (which contains Ca) from the surrounding Ca-rich lime matrix. As such, the total mass of EB used to paint the room was estimated according to Eq. (1) (see the “Methods” section).

The surface area of blue regions was measured for each architectural element in the room (Supplemental Table S1). From VIL imaging (Figs.

5 and 6), we calculated a base layer of EB everywhere above the bottom black sections of the wall. The three red niches (Fig. 3f) displayed signs of mild pigment degradation, with no detectable EB underneath, so they were excluded from the surface area calculations. The repeating pattern on the cornice (Fig. S8) was estimated to contain 50% EB. Summing the base wall and cornice areas, while subtracting the red niche areas, yielded a total EB-covered surface area of 19.92 m^2 .

The mean thickness of the blue pigment layer was determined to be $185 \pm 29\text{ }\mu\text{m}$ from fifteen measurements spaced along the cross-section (Fig. S9). Since minimal sampling was undertaken to preserve the Pompeian materials, the embedded section (BR03) was used to approximate the thickness of the EB layer across the room. For comparison, in the *House of the Colored Capitals* (also referred to as the *House of Ariadne*), the thickness of the EB layer was $75\text{ }\mu\text{m}$ ¹². The difference between 185 and $75\text{ }\mu\text{m}$ is minimal (only a tenth of a millimeter), especially considering the frescoes were hand-painted; however, the thickness value does impact the volume estimation of the pigment layer: Surface area EB painted surface area (19.92 m^2) \times average EB-containing layer thickness ($185\text{ }\mu\text{m}$) = pigment layer volume (3685.2 cm^3).

To determine the percentage of EB, ImageJ (Analyze and Measure functions) was used to isolate the Cu-rich particles and calculate their total area fraction.

In VF1 (Fig. 11a), we used an isolated Cu map of the un-embedded wall section (BR02 Fig. 9, column d middle) for analysis. After noise filtering and binarizing, ImageJ returned a 33.62% Cu area fraction. Returning to the raw reference pigment sections (Fig. 8), we recall the ratio of 76.56% Cu-containing phases and 23.44% non-Cu contributions (1:0.306 ratio). If 33.62% of the BR02 map is Cu-containing, then this reference ratio allows us

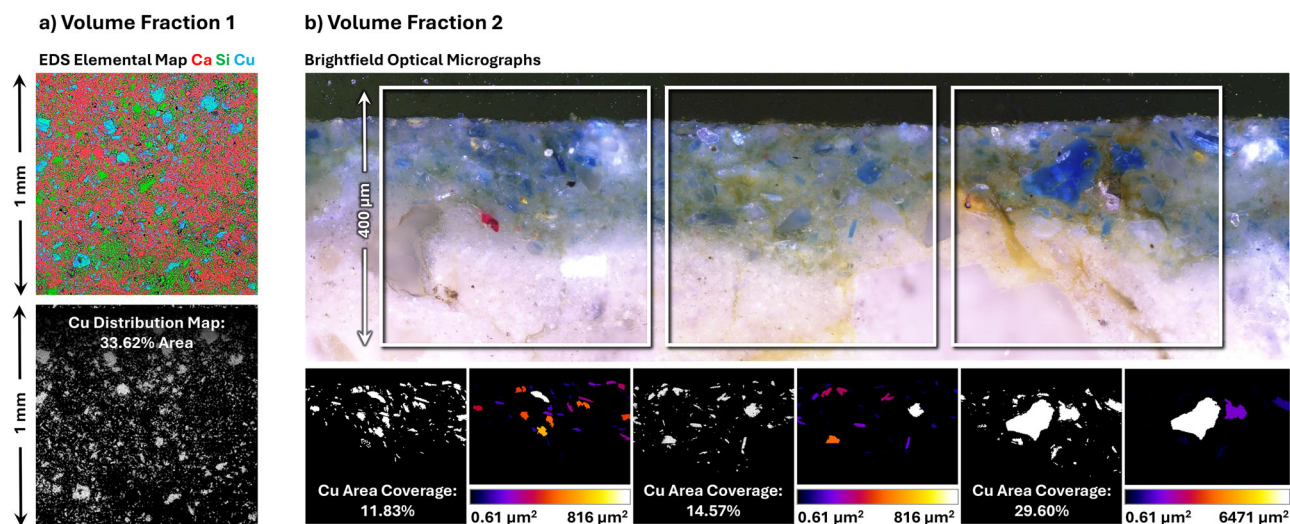


Fig. 11 | Volume fraction calculations for Cu-containing domains. **a** Top: EDS elemental map of BR02 (Ca, Si, Cu); bottom: isolated Cu signal showing 33.62% area coverage. **b** Top row: brightfield optical micrograph of BR03, with three regions

boxed in white; bottom row: corresponding binarized Cu maps with particle size distribution color-coded for clarity (*Biovoxxel* FIJI plugin). The percent coverage of Cu-rich areas is reported for each region.

to include the theoretical non-Cu phases: $33.62\% \times (1_{\text{from Cu}} + 0.306_{\text{from Non-Cu}}) = 43.91\%$ EB contribution.

In VF2 (Fig. 11b), the Cu-contribution of three $400 \mu\text{m} \times 400 \mu\text{m}$ elemental maps was de-noised, binarized, and subsequently cropped, using the optical image as a guide, to encompass just the area of the blue pigment layer. The ratio of Cu area: total area for each region (bottom row) returned Cu area fractions of 11.83%, 14.57%, and 29.60%, with an average Cu-containing area fraction of 18.67%. This percentage was similarly adjusted according to the reference ratio to include the theoretical non-Cu phases: $18.67\% \times (1_{\text{from Cu}} + 0.306_{\text{from Non-Cu}}) = 24.38\%$ EB contribution.

The commonly accepted density of $\text{CaCuSi}_4\text{O}_{10}$ (3.08 g/cm^3) was used to estimate a total mass of EB used to paint the Blue Room: $3685.2 \text{ cm}^3_{\text{EB-Containing Layer Volume}} \times 3.08 \text{ g/cm}^3_{\text{density}} \times \text{VF}_{1,2} = \text{EB mass (g)}$.

By using these approximations, we estimate that with VF1 (43.91%), a total quantity of 4984 g of EB was used in the production of the *Blue Room*, and with VF2 (24.38%), 2767 g of EB was used. We simplify these bounds as 4.9 kg (upper) and 2.7 kg (lower).

EB and other ancient pigment prices

Ancient authors such as Pliny the Elder, Vitruvius, Theophrastus, and Diocletian wrote about EB, offering valuable insights into its composition, quality, and price⁴⁵. Pliny the Elder, writing in the 1970s CE near Naples, provides the most detailed account of blue pigments in the early Roman Empire in his work *Naturalis Historia* (NH)⁴⁶. However, we recognize that prices may have varied across the empire depending on transport distance, merchant control, local supply, and bargaining power. Therefore, we use Pliny's records as a general indication of value, while understanding that they represent only one point within a complex economic landscape.

To estimate the cost of EB used in the production of the *Blue Room*, we draw from Pliny's discussion of several blue colorants: *armenium*, *indicum*, *caeruleum*, *lomantum*, and *cylon*¹⁹. For *caeruleum*, which Pliny uses as a general term for blue, he adds distinctions using provenance through the suffixes *Aegyptios*, *Cyprium*, *Puteolanum*, *Scythicum*, and *Vestorianum*^{1,19}. Some of these blues refer to EB variants, while others do not. For example, the non-EB pigments include azurite as *armenium* (which Pliny also refers to as *caeruleum Cyprium* in NH 33.57 and 33.12), lazurite as *caeruleum Scythicum* (NH 33.57), and indigo as *indicum* (NH 35)^{19,47}. For the general *caeruleum*, Pliny specifies that it is 8 denarii per libra (1 Roman libra (Roman pound) = 327 g⁴⁸ = 0.72 modern pounds), commonly applied to clay surfaces, and unsuitable for lime-based application, making this blue

unlikely to be the material used in the *Blue Room* (for lime-based frescoes). Prior studies suggest that this *caeruleum* is actually a dye⁴⁵.

The EBs described by Pliny in NH 33.57 include *caeruleum Aegyptios* (from Egypt), *caeruleum Puteolanum* (from Puteoli, also referred to as *cylon*, *coelon*, or *cyanon*), and *caeruleum Vestorianum* (produced near the Bay of Naples and made from the 'finer parts' of *caeruleum Aegyptios*)¹. Pliny then describes a washed and finely ground form of *caeruleum*, called *lomantum*, which had a paler hue and cost 10 denarii per libra (NH 33.57). He also mentions a much cheaper variant of *lomantum*, just 0.31 denarii per libra, obtained through prolonged washing and grinding of EB⁴⁹. *Caeruleum Vestorianum*, priced at 11 denarii per libra, is the most likely candidate for the EB found in the *Blue Room*.

To contextualize EB against the cost of other pigments, Pliny records that the highest-quality ocher ("Attic sil") sold for 2 denarii per libra, orpiment for up to 4 denarii per libra, chrysocolla for 3–7 denarii per libra, and indicum for as much as 17 denarii per libra⁵⁰. In NH Book 35, he also lists the *colores floridi*, the most rare and prestigious pigments, including minium, cinnabaris, chrysocolla, purpurissum, as well as the two blues *armenium* and *indicum*¹. Pliny notes that pigments of this expense were typically supplied by the patron commissioning the work, rather than by the painter. This context suggests that while EB was valuable, it was not priced as highly as pigments like *indicum*, though it was considered more costly than chrysocolla, itself one of the *colores floridi*. Notably, merchants in Pompeii may have sold EB pre-mixed with calcite or aragonite chalk¹⁷, which may have affected pricing.

Blue Room cost approximation and contextualization

To estimate the economic investment required for the *Blue Room*'s decoration, we consider the price of EB at 11 denarii per libra and the total weight of pigment used between 2767 and 4984 g. This mass yields a cost range of 93–168 denarii for the EB pigment alone.

To contextualize this amount of denarii in daily Roman life, a loaf of bread during the first and second centuries AD cost approximately 0.0625–0.125 denarii (1/16th–1/8th of a denarii)⁵¹. In the city, a loaf of bread would have been priced at ca. 0.125 denarii⁵². This means, using the more expensive city price, the cost of the EB in the *Blue Room* was equivalent to roughly 744 to 1344 loaves of bread. For further context, at the time of the eruption of Vesuvius, a Roman foot soldier would have been paid ~187 denarii per year⁵³, making our conservative estimate of pigment cost between 50% and 90% of this annual income.

Discussion

Previous studies have attempted to estimate the mass of pigment used in artwork containing EB. For example, Hatton et al.^{15,54} suggested that one gram of EB covers 17.5 cm² of surface area, which, applied to the *Blue Room* suggests upwards of 11 kg of EB would have been used to paint the space. While the specific particle density in the Hatton et al. experiments is unknown, the work was based on replications of Egyptian wall paintings (tomb of Queen Nefertari at Thebes and the temple at Medinat Habu), which likely display deeper, more saturated blues than the lighter-blue Pompeian frescoes with sparser EB application. Another experiment, recreating Roman wall paintings using the frescoes of Saint Savin as a reference, documented that 100 g of pigment per m² was sufficient for coverage⁵⁵. Although not specific to EB, this value has been applied in a previous study to estimate EB use in the *House of the Painters at Work*⁵⁵. Applying this estimate to the *Blue Room* yields a value of ca. 2 kg of EB. While these previous studies were largely based on qualitative estimates, our present study (which estimated 2.7–4.9 kg of EB) introduces a more rigorous quantitative approach that incorporates both elemental mapping and cross-sectional analysis, moving closer to a more accurate estimation of EB use in the *Blue Room*.

Among blue pigments used in Roman wall paintings, EB was the most common, while azurite, indigo, and lazurite were rare¹⁹. Evidence from the town of Sant’Omobono in Rome demonstrates that pigments were sold by specialists known as *pigmentarii*⁵⁶. Once materials were secured, wall painting required the division of labor amongst individuals responsible for different aspects of the decorative scheme. For example, the Edict of Maximum Prices (issued in 301 CE by Diocletian) distinguishes between *pictores parietarii* (painters responsible for architectural decoration) and *pictores imaginarii*, who specialized in figural and mythological elements, likely earning higher wages⁵⁷. However, since the Edict postdates Pompeii by multiple centuries, it is difficult to use any of the prices listed as relevant comparisons (for example, the price of EB is listed as a maximum 150 denarii per Roman pound in 301 CE but by that time, prices in general had risen⁵⁸).

Nonetheless, labor likely constituted a major component of wall painting costs. A prior study estimates that manually grinding 7 g of pigment required ~0.08 h⁵⁵. Scaling up to 2.7–4.9 kg of pigment suggests that 31–56 labor hours alone could have been spent on grinding the EB for the *Blue Room*. Regarding the actual painting, fresco work involved multiple stages of plastering. At the Casa dei Pittori al Lavoro, for example, four plaster layers were observed: a rough rendering coat (*trullisatio*), two intermediate *arriccio* layers, and a final fine *intonachino* (Fig. S10)³⁶. These layers had to be applied and dried until the last wet painting layer, requiring coordination between plasterers, pigment grinders, and artists, although we remain unsure of whether laborers were all paid the same (e.g., skilled painters vs. unskilled laborers for plastering)⁵⁵.

Beyond its significance in Pompeii, EB (being one of the most studied pigments of antiquity)¹ has played a critical role in advancing our understanding of archeological pigments. One of the earliest scientific characterizations of any archeological material involved samples of EB from Pompeii, studied by Jean-Antoine Chaptal in 1809 and then Sir Humphry Davy in 1814⁴⁰, and ongoing investigations into the *domus* in *Regio IX*, where the *Blue Room* is located, continue to offer valuable insights into Pompeian domestic life before the eruption of Mt. Vesuvius.

The findings from the *Blue Room* offer direct insight into the extensive use and economic significance of EB in Pompeii. Through the combined use of portable VIL imaging, optical microscopy, Raman spectroscopy, and SEM-EDS, this multi-spectral study confirmed that the blue pigment was applied in the fresco technique as a solid base layer beneath red, yellow, and white pigments. In the *Blue Room*, we see a sky-blue hue similar to that found elsewhere in Pompeii, but the quantity of EB employed is markedly greater than usual, since the entire background of all three walls is painted with it, rather than limiting its use to a specific decorative element. The range for the quantity of EB used to paint the room, from 2.7 to 4.9 kg and costing 93–168 denarii, underscores the considerable expense involved in its application. We estimated that this pigment cost was equivalent to hundreds of bread loaves in

ancient Rome, or from half to double the yearly salary of a Roman foot soldier. As mentioned above, this figure represents solely the cost of the raw EB material, and the creation of the *Blue Room* would have also included expenses from other pigments, fresco materials, and labor costs from the artists.

The *Blue Room* is one of the smallest rooms in the entire *domus*, and based on its apparent secondary function as a storage room leading up to the eruption, it was not even the most important room of the complex. While the use of EB as a base layer across the entire shrine could be interpreted as a reduction in the perceived value of EB, we suggest that this choice by the owners speaks less to the value of the pigment and more to the substantial wealth of the household.

The presence of EB in a private shrine within a lavish *domus* reinforces the idea that this pigment is featured in the personal, elite environments of Pompeii’s wealthier residents. This artistic practice aligns with broader trends in the Roman economy, where luxury pigments were used to signal status and cultural refinement. As demonstrated in the case of the *Blue Room* described here, this study clearly highlights the role of non-invasive and minimally invasive techniques in preserving cultural heritage while uncovering further details about the polychromatic lives of Pompeians. With approximately one-fourth of Pompeii still unexcavated, methods like portable (ambient light) VIL imaging have proved critical for identifying pigments without destructive sampling, and with more widespread use could further deepen our understanding of art, culture, technology, and the economy in the ancient world.

Data availability

All data needed to evaluate the conclusions in the paper are present in the paper and/or the Supplementary Information. No public repository deposition of data is possible due to legal and ethical restrictions associated with the archeological context and cultural heritage protections governing the study area. These data include archeological material and sample information belonging to the Archeological Park of Pompeii, which are subject to national heritage laws and site-specific access regulations. Access to the data is restricted but can be requested by contacting Dr. Valeria Amoretti (valeria.amoretti@cultura.gov.it) and Dr. Antonino Russo (antonino.russo@cultura.gov.it). Requests will be evaluated by the Pompeii Archeological Sites according to their data sharing and permissions policy.

Code availability

The underlying code for this study is not publicly available but can be made available upon request.

Received: 26 May 2025; Accepted: 22 January 2026;

Published online: 03 March 2026

References

- Nicola, M., Gobetto, R. & Masic, A. Egyptian blue, Chinese blue, and related two-dimensional silicates: from antiquity to future technologies. Part A: general properties and historical uses. *Rend. Lincei Sci. Fis. E Nat.* **34**, 369–413 (2023).
- Stodd, D. A. A review of ancient Egyptian pigments and cosmetics. *Stud. Conserv.* **61**, 185–202 (2016).
- Skovmøller, A., Brøns, C. & Sargent, M. L. Egyptian blue: modern myths, ancient realities. *J. Roman Archaeol.* **29**, 371–387 (2016).
- Švarcová, S., Hradil, D., Hradilová, J. & Čermáková, Z. Pigments—copper-based greens and blues. *Archaeol. Anthropol. Sci.* **13**, 190 (2021).
- Kovalev, I., Rodler, A. S., Brøns, C. & Rehren, T. H. Making and working Egyptian blue—a review of the archaeological evidence. *J. Archaeol. Sci.* **153**, 105772 (2023).
- Eastaugh, N., Walsh, V., Chaplin, T. & Siddall, R. *Pigment Compendium* (Elsevier Butterworth-Heinemann, 2004).
- Riederer, J. Egyptian blue. In *Artists Pigments: A Handbook of Their History and Characteristics* Vol. 3 (ed. West Fitzhugh, E.) (Oxford University Press, 1997).

8. Corcoran, L. The color blue as an ‘animator’ in ancient Egyptian art. In *Essays in Global Color History: Interpreting the Ancient Spectrum* (ed. Goldman, R. B.) 41–63 (Gorgias Press, 2016).
9. Shortland, A. J. *Lapis Lazuli from the Kiln: Glass and Glassmaking in the Late Bronze Age* (Leuven University Press, 2012).
10. Nicola, M. et al. Increased NIR photoluminescence of Egyptian blue via matrix effect optimization. *Mater. Chem. Phys.* **313**, 128710 (2024).
11. Caggiani, M. C., Colombari, P., Bellot-Gurlet, L., Mazzoleni, P. & Barone, G. Vitruvius-like synthesis of Egyptian Blue using Roman coins as copper source. *Spectrochim. Acta A Mol. Biomol. Spectrosc.* **336**, 126029 (2025).
12. García-Fernández, P., Moreno, M. & Aramburu, J. A. Origin of the exotic blue color of copper-containing historical pigments. *Inorg. Chem.* **54**, 192–199 (2015).
13. McCloy, J. S. et al. Assessment of process variability and color in synthesized and ancient Egyptian blue pigments. *Npj Herit. Sci.* **13**, 202 (2025).
14. Kostomitsopoulou Marketou, A. The materialisation of colour: reconstructing Egyptian blue manufacture on late Hellenistic Kos. *Nor. Archaeol. Rev.* **55**, 21–37 (2022).
15. Hatton, G. D., Shortland, A. J. & Tite, M. S. The production technology of Egyptian blue and green frits from second millennium BC Egypt and Mesopotamia. *J. Archaeol. Sci.* **35**, 1591–1604 (2008).
16. Cappelletti, P. et al. The Roman villa at the Castle of Baia (Naples, Italy): investigations on the polychromy of frescoed surfaces by using non-destructive spectroscopic techniques. *Herit. Sci.* **12**, 328 (2024).
17. Thiboutot, G. *Egyptian Blue in Romano-Egyptian Mummy Portraits* (J. Paul Getty Museum, 2020).
18. Grifa, C. et al. Beyond Vitruvius: new insight in the technology of Egyptian Blue and Green Frits. *J. Am. Ceram. Soc.* **99**, 3467–3475 (2016).
19. Becker, H. Pigment nomenclature in the ancient Near East, Greece, and Rome. *Archaeol. Anthropol. Sci.* **14**, 20 (2022).
20. Prieto-Taboada, N. et al. Understanding the degradation of the blue colour in the wall paintings of Ariadne’s house (Pompeii, Italy) by non-destructive techniques. *J. Raman Spectrosc.* **52**, 85–94 (2021).
21. Piovesan, R., Siddall, R., Mazzoli, C. & Nodari, L. The Temple of Venus (Pompeii): a study of the pigments and painting techniques. *J. Archaeol. Sci.* **38**, 2633–2643 (2011).
22. Miriello, D. et al. Pigments Mapping On Two Mural Paintings of the ‘House of Garden’ in Pompeii (Campania, Italy) <https://doi.org/10.5281/ZENODO.4574643> (2021).
23. Germinario, C. et al. Multi-analytical and non-invasive characterization of the polychromy of wall paintings at the Domus of Octavius Quartio in Pompeii. *Eur. Phys. J. Plus* **133**, 359 (2018).
24. Verri, G., Saunders, D., Ambers, J. & Sweek, T. Digital mapping of Egyptian Blue: conservation implications. *Stud. Conserv.* **55**, 220–224 (2010).
25. Nicola, M. et al. Real-time identification and visualization of Egyptian blue using modified night vision goggles. *Rend. Lincei Sci. Fis. E Nat.* **35**, 495–512 (2024).
26. Zuchtriegel, G. et al. I cantieri antichi di Pompei tra emergenza e ordinaria manutenzione: nuovi dati dall’Insula 10, Regio IX. *Scavi di Pompei*. (2024).
27. Zuchtriegel, G. et al. L’età della nostalgia: il sacrario nella Regio IX, insula 10 di Pompei. *Scavi di Pompei*. **15**, 1–27 (2024).
28. Germinario, C. et al. Roman technological expertise in the construction of perpetual buildings: new insights into the wall paintings of a banquet scene from a tomb in Cumae (southern Italy). *Archaeol. Anthropol. Sci.* **14**, 181 (2022).
29. Grifa, C. et al. Pompeian pigments. A glimpse into ancient Roman colouring materials. *J. Archaeol. Sci.* **177**, 106201 (2025).
30. Verri, G. In *The Application of Visible-induced Luminescence Imaging to the Examination of Museum Objects* (eds. Pezzati, L. & Salimbeni, R.) 739105 (SPIE, 2009).
31. Triolo, P. A. M., Spingardi, M., Costa, G. A. & Locardi, F. Practical application of visible-induced luminescence and use of parasitic IR reflectance as relative spatial reference in Egyptian artifacts. *Archaeol. Anthropol. Sci.* **11**, 5001–5008 (2019).
32. Linn, R., Tepper, Y. & Bar-Oz, G. Visible induced luminescence reveals invisible rays shining from Christ in the early Christian wall painting of the Transfiguration in Shivta. *PLoS ONE* **12**, 1–16 (2017).
33. ASTM. *E562-19e1: Standard Test Method for Determining Volume Fraction by Systematic Manual Point Count* (ASTM, 2020).
34. Iovino, G., Marchello, A., Trapani, A. & Zuchtriegel, G. La disciplina dell’odiosa baracca: la casa con il panificio di Rustio Vero a Pompei (IX 10,1) (*Scavi di Pompei*, 2023).
35. Scappaticcio, M. C. & Zuchtriegel, G. ‘Hic et ubique’: voci e vite nel ‘Salone Nero’ (Regio IX, insula 10) (*Scavi di Pompei*, 2024).
36. Salvadori, M. & Sbrolli, C. Wall paintings through the ages: the Roman period—Republic and early Empire. *Archaeol. Anthropol. Sci.* **13**, 187 (2021).
37. Boschetti, C. Vitreous materials in early mosaics in Italy: Faience Egyptian Blue, and Glass. *J. Glass Stud.* **53**, 59–91 (2011).
38. Arletti, R., Quartieri, S. & Vezzalini, G. Glass mosaic tesserae from Pompeii: an archeometrical investigation. *Period. Mineral.* **76**, 25–38 (2006).
39. Clarke, J. R. *The Houses of Roman Italy, 100 B.C.–A.D. 250: Ritual, Space, and Decoration* (University of California Press, 1991).
40. Pradell, T., Salvado, N., Hatton, G. D. & Tite, M. S. Physical processes involved in production of the ancient pigment, Egyptian Blue. *J. Am. Ceram. Soc.* **89**, 1426–1431 (2006).
41. Dariz, P. & Schmid, T. Trace compounds in Early Medieval Egyptian blue carry information on provenance, manufacture, application, and ageing. *Sci. Rep.* **11**, 11296 (2021).
42. Tite, M. S. Characterisation of early vitreous materials. *Archaeometry* **29**, 21–34 (1987).
43. Pagès-Camagna, S., Colinart, S. & Coupry, C. Fabrication processes of archaeological Egyptian blue and green pigments enlightened by Raman microscopy and scanning electron microscopy. *J. Raman Spectrosc.* **30**, 313–317 (1999).
44. Zenebe, C. G. A review on the role of wollastonite biomaterial in bone tissue engineering. *BioMed. Res. Int.* **2022**, 4996530 (2022).
45. Kakoulli, I. & Balonis, M. Ancient binders and pigments. In *Handbook of Archaeological Sciences* (eds Pollard, A. M., Armitage, R. A. & Makarewicz, C. A.) 833–865 (Wiley, 2023).
46. Becker, H. Grading for colour: Pliny’s hierarchy of pigment quality. In *The Nature of Art: Pliny the Elder on Materials* (eds. Anguissola, A. & Grüner, A.) (Brepols, 2020).
47. Clegg, S. *Blue Shade Hues: A Study of Blue Pigments Used by Romano-British Wall-Painters*. Doctoral thesis, University of Sussex (2014).
48. Robens, E., Jayaweera, S. A. A. & Kiefer, S. *Balances: Instruments, Manufacturers, History* (Springer, 2014).
49. Osanna, M. & Rescigno, C. Il blu egizio in età classica: fonti e testimonianze. *Atti Conv. Lincei* **33**, 51 (2022).
50. Pliny the Elder. Book 33. In *Natural History* Ch. 57 (Perseus Digital Library, Tufts University, 1855).
51. Bowes, K. Tracking consumption at Pompeii: the graffiti lists. *J. Roman Archaeol.* **34**, 552–584 (2021).
52. Bernard, S. Slavery, prosperity, and inequality in Roman Pompeii. *Past Present* gtaf006 <https://doi.org/10.1093/pastj/gtaf006> (2025).
53. Speidel, M. A. Roman army pay scales. *J. Roman Stud.* **82**, 87–106 (1992).
54. Hatton, G. D. *The Technology of Egyptian Blue* (University of Oxford, 2005).
55. Bologna, F. Water and stone: the economics of wall-painting in Pompeii (A.D. 62–79). *J. Roman Archaeol.* **32**, 97–128 (2019).
56. Becker, H. Technology and trade. In *A Cultural History of Color in Antiquity* (ed. Wharton, D.) (Bloomsbury Publishing, 2021).

57. Esposito, D. The economics of Pompeian painting. In *The Economy of Pompeii* (eds. Flohr, M. & Wilson, A) (Oxford University Press, 2017).
58. Svoboda, E. M. & Cartwright, C. R. *Mummy Portraits of Roman Egypt* (APPEAR (Ancient Panel Paintings: Examination, Analysis, and Research), 2013).

Acknowledgements

We acknowledge Parimala Rajesh, Jayna Ekermann, and Ellie Vaserman for assistance with VIL imaging and subtraction. We also thank Dr. Will Gilstrap from the MIT Center for Materials Research in Archaeology and Ethnology (CMRAE) for assistance with sample preparation and the MIT Department of Materials Science and Engineering (MIT DMSE) Breakerspace for use of the Olympus DSX1000 optical microscope.

Author contributions

Designed research: M.N., G.Z., and A.M. Performed research: M.A.Q., J.C.W., and C.G. Contributed new reagents/analytic tools: M.N., J.C.W., C.G., and A.M. Analyzed data: M.A.Q., J.C.W., C.G., M.J.T., and A.M. Wrote the paper: M.A.Q. and A.M. Reviewed and edited the manuscript: M.A.Q., M.N., J.C.W., C.G., V.A., A.R., G.Z., M.J.T., and A.M.

Funding

Open Access funding provided by the MIT Libraries.

Competing interests

The authors declare no competing interests.

Additional information

Supplementary information The online version contains supplementary material available at <https://doi.org/10.1038/s40494-026-02349-2>.

Correspondence and requests for materials should be addressed to Admir Masic.

Reprints and permissions information is available at <http://www.nature.com/reprints>

Publisher's note Springer Nature remains neutral with regard to jurisdictional claims in published maps and institutional affiliations.

Open Access This article is licensed under a Creative Commons Attribution-NonCommercial-NoDerivatives 4.0 International License, which permits any non-commercial use, sharing, distribution and reproduction in any medium or format, as long as you give appropriate credit to the original author(s) and the source, provide a link to the Creative Commons licence, and indicate if you modified the licensed material. You do not have permission under this licence to share adapted material derived from this article or parts of it. The images or other third party material in this article are included in the article's Creative Commons licence, unless indicated otherwise in a credit line to the material. If material is not included in the article's Creative Commons licence and your intended use is not permitted by statutory regulation or exceeds the permitted use, you will need to obtain permission directly from the copyright holder. To view a copy of this licence, visit <http://creativecommons.org/licenses/by-nc-nd/4.0/>.

© The Author(s) 2026